Lab on a Chip

PAPER

View Article Online
View Journal | View Issue

Cite this: *Lab Chip*, 2015, **15**, 1116

Microfluidic devices for imaging neurological response of *Drosophila melanogaster* larva to auditory stimulus†

Reza Ghaemi,[a] Pouya Rezai,[ab] Balaji G. Iyengar[ac] and Ponnambalam Ravi Selvaganapathy*[a]

Two microfluidic devices (pneumatic chip and FlexiChip) have been developed for immobilization and live-intact fluorescence functional imaging of *Drosophila* larva's Central Nervous System (CNS) in response to controlled acoustic stimulation. The pneumatic chip is suited for automated loading/unloading and potentially allows high throughput operation for studies with a large number of larvae while the FlexiChip provides a simple and quick manual option for animal loading and is suited for smaller studies. Both chips were capable of significantly reducing the endogenous CNS movement while still allowing the study of sound-stimulated CNS activities of *Drosophila* 3rd instar larvae using genetically encoded calcium indicator GCaMP5. Temporal effects of sound frequency (50–5000 Hz) and intensity (95–115 dB) on CNS activities were investigated and a peak neuronal response of 200 Hz was identified. Our lab-on-chip devices can not only aid further studies of *Drosophila* larva's auditory responses but can be also adopted for functional imaging of CNS activities in response to other sensory cues. Auditory stimuli and the corresponding response of the CNS can potentially be used as a tool to study the effect of chemicals on the neurophysiology of this model organism.

Received 20th October 2014,
Accepted 11th December 2014

DOI: 10.1039/c4lc01245c

www.rsc.org/loc

1. Introduction

Drosophila melanogaster is a widely used model organism for studying human biology and diseases at the molecular-genetic level.[1–3] This is due to its many advantages such as molecular-genetic, developmental, cellular/neuronal simplicity, genetic tractability and the increasingly incisive application of advanced optical methods for live imaging of biological processes. At its larval stages, *Drosophila* contains different types of sensory neurons that are patterned in a segmental configuration. They sense various environmental cues (*e.g.* mechanical, visual and chemical) and relay information to the Central Nervous System (CNS) to help elicit stereotypic motor behaviors. This simple architecture continues to be exploited for studying numerous developmental-genetic and neurobiological problems primarily through deploying surgical, histological, transgenic and behavioral methods.[4,5]

Studying the behavioral responses in the larval stage of *Drosophila* using neuroimaging methods is challenging because the larva exhibits robust digging and burrowing behavior. This behavior is carried out by a cylindrical body wall that contains segmentally iterated sets of skeletal muscles and a specialized structure at the anterior end called the cephalopharyngeal skeleton (CPS). The latter is operated by specialized muscles to enable digging into food substrates.[6] This digging movement is an impediment to temporal imaging of fluorescence activities in the larval sensory neurons and the CNS (see the ESI† S2). Conventional immobilization methodologies involving the use of anesthetic drugs will affect animals' neurophysiological status.[7] Other methods, such as the use of tissue glue, used to immobilize embryos are irreversible, use solvents that could affect the physiological state and do not completely immobilize the CNS. Ideally, immobilization has to be performed in a simple and reversible manner while still allowing sensory stimulus to affect the larva. Miniaturized microfluidic devices are best suited for this purpose.

Microfabricated lab-on-chip devices are increasingly being used in the study of various model organisms such as *Caenorhabditis elegans*[8,9] and *Drosophila*[10–12] as they enable automated immobilization of these small organisms. After immobilization, visualization and tracking of cellular and physiological responses *in vivo* can be performed through their transparent body wall without motion artifacts. Microfluidic-based immobilization techniques for *C. elegans*

[a] *Department of Mechanical Engineering, McMaster University, Hamilton, ON, Canada. E-mail: selvaga@mcmaster.ca*
[b] *Department of Mechanical Engineering, York University, Toronto, ON, Canada*
[c] *Qiptera Solutions Inc. McMaster Innovation Park, Hamilton, ON, Canada*
† Electronic supplementary information (ESI) available. See DOI: 10.1039/c4lc01245c

have been developed using chemical (CO_2) or mechanical (tapering microchannels or encapsulation using deflectable PDMS membranes) approaches.[13–16] In the case of *Drosophila*, microfluidic devices have also been recently developed mostly to automate the embryo assays[17,18] (self-assembly of eggs and morphogenesis,[19,20] developmental studies[21] and injection[19,22]) and less attention has been given to on-chip larval studies. Immobilization of *Drosophila* larvae is more difficult than that of *C. elegans* as it exerts stronger force. Complicating matters further, the internal organs of interest such as the CNS capsule that needs to be visualized can loosely move inside the hemolymph-filled body cavity even if the outer body is completely immobilized by encapsulation. Recently, mechanical encapsulation[10] and CO_2 anesthetic exposure[11] approaches have been used to immobilize *Drosophila* larva. They allow whole-larval body compression inside the chip so that neuronal transport processes[10] and sensory neuron regeneration upon injury[11] can be visualized. Both these devices reduce the movement artifacts as compared to the freely moving larva but do not eliminate them. The use of anesthetic leads to spurious neurobehavioral responses and the use of encapsulation prevents the exposure of the larva to external sensory stimulus.

Very recently, behavioral responses of *Drosophila* larva in reaction to mechanical stimuli (vibration and sound) have been studied.[23,24] Zhang *et al.*[23] used Ca^{2+} imaging and electrophysiological methods and found that *Drosophila* larvae's Cho and class IV DA neurons responded optimally to sound waves at 500 Hz frequency. In these studies, the immobilization for Ca^{2+} imaging was achieved by compressing the larvae (in saline) between coverslips. This is a manual process and the degree of compression, the access of the larva to the external stimuli and the orientation of the animal are all variable and dependent on the operator. It is also conceivable that the overt whole-body mechanical compression could be disruptive for the full range of endogenous sensory-motor activities to take place.

In this paper, we demonstrate two lab-on-chip designs that standardize the immobilization of the larva while still allowing access to external stimuli and for the first time, conduct an on-chip study of the CNS activity of *Drosophila* larvae evoked by acoustic signals. The use of acoustic signals enabled fast, automated, remote and tunable stimulation of specimens. Specifically we investigated these responses fluorescently at the ventral cord of the CNS, an anatomical structure where a large majority of sensory afferents synapse with interneurons. We expressed a new genetically encoded calcium sensor GCaMP5 (ref. 25) in all sensory and cholinergic interneurons. Our devices are engineered to stabilize the CNS specifically from ongoing motor movements and the resulting internal hemolymph displacements. We demonstrate that localized anchoring of the larval CPS permits functional imaging of CNS in response to auditory stimuli. Our larval-lab-on-a-chip platforms will also be useful for studying CNS responses to other sensory cues (light, chemosensory, tactile, electric/magnetic fields).

2. Methods

The neurological response of *Drosophila* larvae to auditory stimuli was studied using two different lab-on-chip designs. Device design and fabrication, experimental procedures, data acquisition and processing as well as animal preparation are described in this section.

2.1. Design of the microfluidic chips

Drosophila larva's burrowing and locomotory behaviors make the CNS capsule move inside the hemolymph-filled body cavity because it is loosely anchored (Fig. 1). In order to immobilize the CNS of the larva and to subsequently study its neurological responses to auditory stimulus, two chips, named the pneumatic chip and the FlexiChip, were designed.

2.1.1. Pneumatic chip. The pneumatic chip was designed for automated loading, immobilization, testing and unloading of the animals. The first chip (schematically shown in Fig. 2) consisted of an inlet port for animal loading into the device, a channel (inlet in Fig. 2) for transporting the animal towards

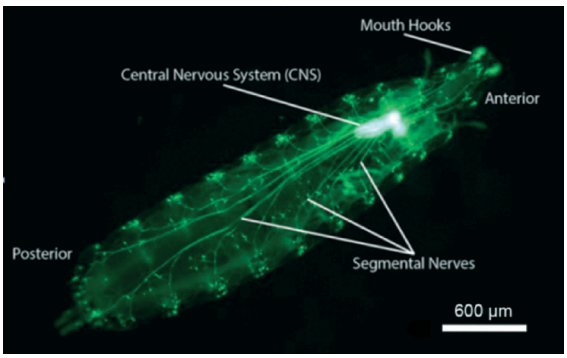

Fig. 1 Epifluorescence image of a 3rd instar larva expressing GFP in all cholinergic neurons as driven by Cha-Gal4, UAS-GFP transgenes. The Central Nervous System (CNS) zone is indicated, and its neuronal activity was monitored by expressing a UAS-GCaMP5 transgene.

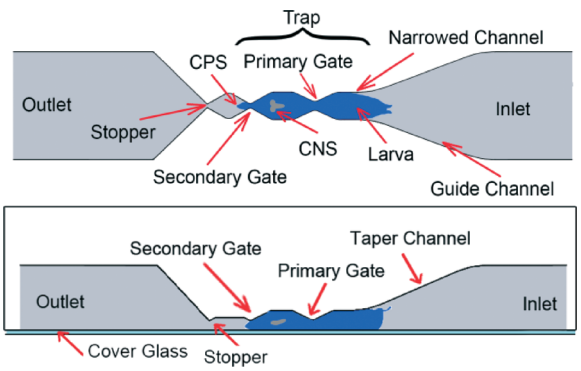

Fig. 2 Schematic design of the pneumatic chip (not to scale) – top view (top image) and side view (bottom). The inlet channel was 25 mm long, 3 mm wide and 2 mm deep with an inlet port for animal loading located at its end. The outlet channel was 8 mm long, 3 mm wide and 2 mm deep for ejection of tested animals.

the tapered trap that was designed to immobilize the larvae for imaging and an outlet for ejection of the tested animal upon completion of each experiment. The trap consisted of a narrowed channel (770 × 700 μm^2 cross section with 500 μm length), primary (200 μm width and 450 μm depth) and secondary gates (100 μm width and 425 μm depth) and a stopper (100 μm width and 100 μm depth). The primary and secondary gates were designed to pin the 3rd instar larva at two locations on its body while the rest of it was encapsulated in the narrowed channel. We found that without the two-point pinning, the CNS could move longitudinally inside the body despite the complete encapsulation of the larval body in the trap, thereby compromising clear imaging of the neuronal activities in the CNS. The dimensions of the secondary gate were designed such that only the nose region of the immobilized 3rd instar larva could protrude through the gate. This gate was used to prevent the larva from escaping the trap when a small sustained pressure was used on the posterior side for complete immobilization (see section 2.4.1).

2.1.2. FlexiChip. In order to study the influence of the device design on the auditory response of the larvae, another chip (FlexiChip) with different mechanical and acoustic properties that facilitated manual animal loading was used. The schematic of the FlexiChip (Fig. 3) summarizes its basic design and operation. The key features of the FlexiChip were a main channel that fits the 3rd instar larva (similar to the pneumatic chip) and a clasping mechanism (clip) that was designed into the PDMS substrate so as to clamp the head of the larva (Fig. 3). Both features are included into the 3D printed mold. The clip mechanism opens when the PDMS is flexed and closes when the flexion is removed. The clip-gate also contains a 100 μm diameter glass wire on the top to create an enclosed hole or a burrow-like opening that encourages the larva to enter it; the glass wire also stabilized the anchoring upon clip closure. The auxiliary channels are available to keep the preparation moistened, or for the introduction of electrical or mechanical probes for body-wall stimulation. The arrowhead in Fig. 3 indicates the approximate location of the CNS ventral cord (VC) that resides just below the ventral body-wall of the larva so that live-imaging could be carried out, often with almost no extraneous tissue obstruction. The FlexiChip allowed the larva to continue breathing while being subjected to various types of sensory stimulations.

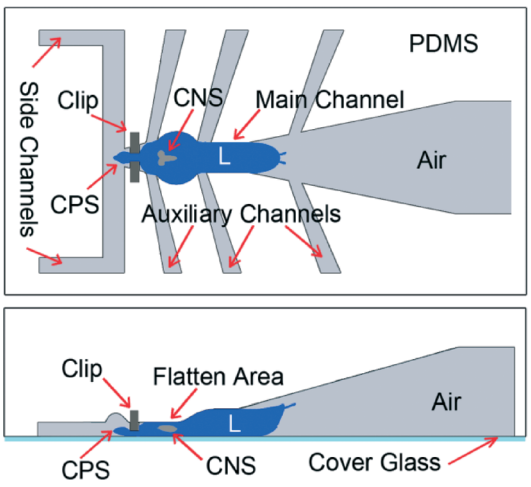

Fig. 3 Schematic design of the FlexiChip (not to scale) – top view (top image) and side view (bottom).

2.2. Device fabrication

Devices were fabricated by 3D printing of two plastic master molds that dimensionally corresponded to the design discussed in section 2.1 for the pneumatic chip and the FlexiChip. Following master mold fabrication, soft lithography[26] was used for conventional PDMS (10 : 1 ratio base : agent, SYLGARD® 184) casting, curing (70 °C, 2 h), bonding to glass slides (80 s, 50 W, plasma oxygen) and installation of inlet/outlet tubes (for pneumatic chip, silicone tubing, 3/16" ID × 5/16" OD, Cole-Parmer Canada Inc.). The glass wire in the FlexiChip was placed into the 3D mold at the location of the clip before casting the PDMS into the mold.

2.3. Experimental setup

The experimental setup (Fig. 4) consisted of a sound-insulated box (custom made to isolate environmental noises using acoustic sound damping foam UL 94, Parts-Express, USA), an acoustic signal generation system (function generator (AFG3022B, Tektronix, CA), amplifier (RAMSA WO-1200, Panasonic, CA) and speaker (Eminence Beta-12CX coaxial 12", Parts-express, USA)), an optical/fluorescence imaging system (Lumascope 500, single color 488 nm Ex. fluorescence, 40× magnification, Etaluma, CA), the microfluidic device and a software control system (LabVIEW©, flyCapture2© and ImageJ© software).

The function generator connected to the amplifier was controlled through a custom LabVIEW© code and was used

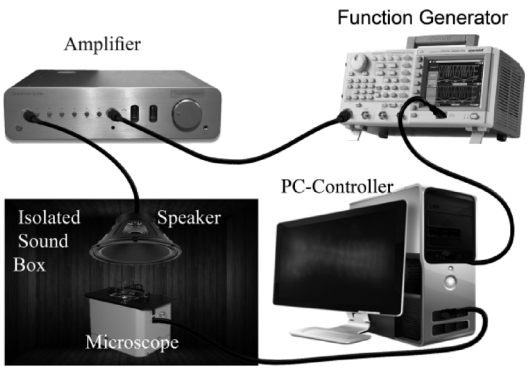

Fig. 4 Experimental setup used to examine the auditory response of *Drosophila* larvae. A sound insulation box with internal walls covered with sound damping foam was used to accommodate the microscope right underneath the speaker. The speaker was connected to a function generator (FG) through an amplifier for sound actuation (sinusoidal voltage output from FG). Both the microscope and the FG were connected to a PC for automated control of image acquisition and signal generation (frequency and peak–peak voltage), respectively.

to generate the desired pure-tone sinusoidal voltage signal inputs to the speaker. The speaker was installed on the roof of the sound insulating box. Various voltage frequency and intensity levels were generated and amplified to the speaker and the corresponding sound frequency (50–5000 Hz) and intensity (95–115 dB) produced in the box were measured using a mini sound level meter (DT-85A, CEM). This was done to calibrate the speaker and the sound insulating box. Frequency ranges were selected to cover the hearing range of the response of *Drosophila*[23] and intensity levels were selected using preliminary experiments that produced a response in the CNS.

The microscope was positioned inside the box right beneath the speaker with a 15 cm distance between its focal plane and the speaker. The microscope was controlled by software and used in the optical mode for loading the animal and in the fluorescence mode for imaging GCaMP5 activities in the CNS of an immobilized larva.

2.4. Animal loading

2.4.1. Pneumatic chip. *Drosophila* larva (3rd instar) was picked from the food medium using a soft brush, washed with DI water and loaded into the chip at the inlet. Then, the larva was pneumatically inserted into the entrance region of the trap (Fig. 5a) in 10 s *via* the inlet channel. The larvae often oriented themselves and crawled voluntarily with no external pressure half-way into the trap up to the primary gate (Fig. 5b–d) which helped in the proper orientation and imaging of the CNS. This could take up to 30 s but robustly produced desired orientations after immobilization. The animal was then pneumatically pushed further inside the trap (using a 0.8 bar continuous pressure) and stopped automatically when the head of the larvae reached the secondary gate in less than 3 s (Fig. 5e). After animal loading and immobilization, a continuous 0.3 bar pressure was applied and maintained at the inlet port to inhibit any further CNS longitudinal movements and to prevent the larva from crawling back and moving out of the trap. The animal was viably kept inside the aqueous environment for the entire duration of the experiment (215 s, see section 2.5). Using the shown configuration, we successfully immobilized the *Drosophila* larva with minimal internal CNS movements for its subsequent live neuronal imaging under various acoustic wave conditions inside the insulating box.

2.4.2. FlexiChip. The loading of the larva into FlexiChip was performed by bending the chip laterally (Fig. 6a, the bending opened the clip (double-headed arrow) (Fig. 6b)) so that the CPS area could be inserted into the gap (arrow in Fig. 6c) with the larva's ventral side facing upwards. When a drop of water was placed at the clamp area the larva automatically attempted to burrow into the clamp area. Release of the bending facilitated the anchoring of the anterior segments of the larva that contains the burrowing apparatus. In addition, a glass wire was used at the top of this clamping area to restrict the movement of the larva in this direction and prevent its escape from the clamp for a longer time.

Afterwards, a cover-glass was placed on top of the larva (Fig. 6d) before visualization of fluorescence activities in the ventral cord aspect of the CNS (see the ESI† S4) where a large majority of afferent sensory inputs from the body wall arrive. The larval posterior-end protruded into a funnel shaped outer chamber that was open to ambient air. This allowed respiration to continue through posterior spiracles during live imaging. The procedure for loading the larva into the chip takes approximately 5 min.

2.5. Automated animal testing

After the animal was properly loaded into the trap and immobilized, as shown in Fig. 5 and 6, the auditory response

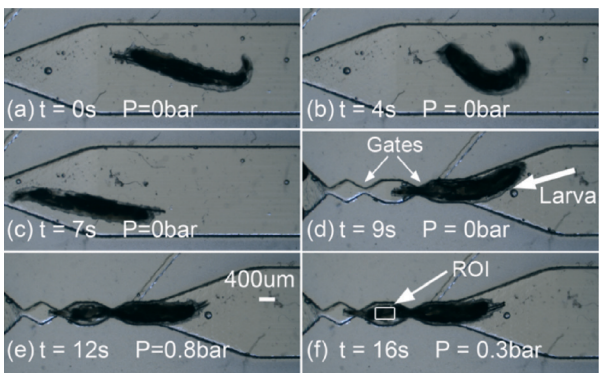

Fig. 5 Steps to load the larva using the pneumatic chip. (a–d) The larva swam freely into the trap, and (e–f) the larva was pneumatically moved into the trap and immobilized. Time-lapsed fluorescence imaging was then conducted on the CNS located inside the Region of Interest (ROI). Scale bar = 400 μm for all figures is shown in Fig. 5e.

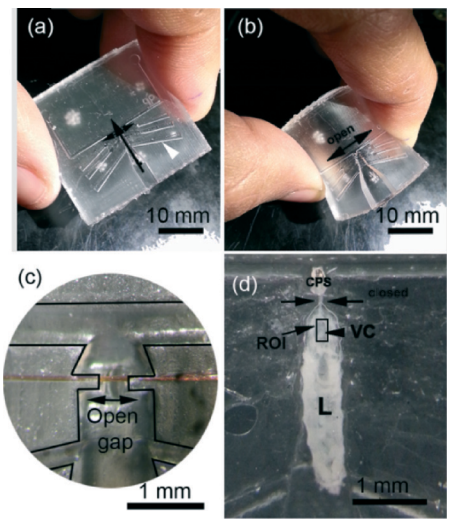

Fig. 6 Steps to load the larva using the FlexiChip. The chip (a) is bent (b) so that the clip (c) opens. Then, the animal is inserted into the gap and the chip is released and sealed by a coverslip (d). Time-lapsed fluorescence imaging was then conducted on the CNS located inside the Region of Interest (ROI).[31]

of the larva was examined at the abdominal ganglia region of the ventral cord. A custom-made LabVIEW© code controlling the function generator was used to generate a step-like periodic series of acoustic waves (5 s on and 5 s off) while the animal's CNS fluorescence signal activities were recorded in a movie format using the microscope. Each on-portion cycle of the applied wave corresponded to one frequency (50, 100, 200, 500, 1000, 2000 or 5000 Hz) and one intensity (95, 105 or 115 dB) level. The experiment was continued automatically until the entire 21 frequency–intensity combinations were tested. The animal was then washed off the chip and another one was loaded to repeat the experiments. The movies were then analysed as discussed below for quantification of neuronal activities.

2.6. Data acquisition and processing

The movies recorded for each animal were analyzed by ImageJ© software (National Institutes of Health, USA) to quantify the fluorescence intensity variations in the CNS in response to the applied acoustic signals. The RGB image sequences for each video were converted to 8-bit black and white images (256 shades of gray). After subtracting the background with a rolling ball radius of 100 pixels, a Region of Interest (ROI in Fig. 5f and 6d) covering the CNS was selected and the mean gray value for the entire image stack was measured inside the ROI and recorded in an Excel file. The intensity variation in each condition was calculated by taking the ratio of the increase in the mean gray value in the ROI during the stimuli to the mean gray value 2 seconds before sound was applied in each experiment.

It is important to note that the inherent movement of the animal also results in an increase in CNS activity that may lead to elevated baseline reading. Movement was measured as the change in the center of mass of the CNS and experiments that had high CNS movement were not included in the analysis.

2.7. Animal preparation

Larvae of the genotype w, Cha-Gal4/CyO; UAS-GCaMP5/TM3, Sb were used for imaging CNS activity in response to auditory stimulations. Heterozygotes and homozygotes were not separated before testing. Expression of the GCaMP5 GECI was conducted using the Gal4/UAS system.[27] Through standard fly crosses, a stable fly stock was created containing two transgenes: (1) Cha-Gal4 is a promoter sequence of choline acetyltransferase (Cha) driving the expression of the Gal4 transcription factor,[28] and (2) UAS-GCaMP5 transgene contains the binding sites for the Gal4 transcription factor.[25] Thus, in the Cha-Gal4/CyO; UAS-GCaMP5/TM3 strain, all sensory and central neurons that express the choline acetyltransferase gene express the GCaMP5 calcium sensor. The GCaMP calcium sensor is a circularly permuted protein containing the Green Fluorescent Protein (GFP), calcium binding protein called calmodulin, and the M13 (calmodulin binding) peptide.[29] Influx of Ca^{2+} during neuronal activity triggers a conformational change of GCaMP so that solvent access to the chromophore is prevented, thus resulting in a higher level of fluorescence.[30] GCaMP5 is a recently developed high signal-to-noise ratio calcium sensor.[25] This genotype was generated through a standard genetic crossing scheme. Third instar stage larvae were isolated using a fine brush, washed with distilled water and dried on a tissue paper before loading into the chips.

3. Results and discussion

3.1 Acoustic response of *Drosophila* 3rd instar larva

After immobilizing the larva (3rd instar) inside each of the PDMS devices, as shown in Fig. 5 and 6, neuronal activities in the CNS in response to a sound wave (5 s duration, 200 Hz frequency and 105 dB intensity) were measured using the experimental setup described before (Fig. 4). We measured the frequency and intensity of the sound inside both of the devices and found them to be the same as those outside. As shown in Fig. 7 (response of the immobilized larva in the pneumatic chip), the animal's CNS activity increased by 21% (reported by an increase in average fluorescence intensity) upon exposure to the sound signal and returned to its original state within 0.5 s after the signal was turned off (image not shown due to similarity to Fig. 7a). This type of response was observed consistently for 5 animals tested under the same acoustic conditions and each time it was tested.

3.2 Investigation of the effect of sound frequency and intensity on *Drosophila* larva CNS activities

The interesting observation of a significant CNS activity in response to a sound signal (Fig. 7) encouraged us to investigate this phenomenon further in detail. Hence, we recorded the CNS activities of *Drosophila* 3rd instar larvae in response to sound signals of various intensity (95–115 dB) and frequency (50–5000 Hz) levels using both the pneumatic chip and the FlexiChip (Fig. 8, averaged for $n = 5$ animals).

As shown in Fig. 8, the animals tested in both chips demonstrated a statistically significant increase in CNS activities when the frequency of the sound signal was increased from 50 Hz to 200 Hz. A further increase in frequency resulted in reduced CNS activities as compared to the 200 Hz condition. In addition to a peak in response at 200 Hz, a secondary but less significant peak in CNS response was also observed at 2000 Hz and only inside the pneumatic chip (Fig. 8a). This peak was more significantly pronounced at higher intensity levels (105 and 115 dB). In contrast, at 95 dB the difference

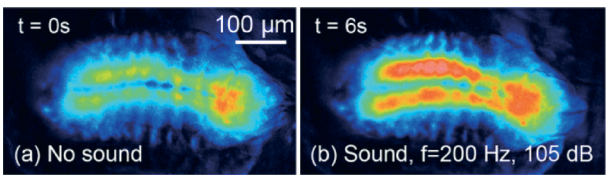

Fig. 7 Snapshots of the fluorescence activities in the CNS of a larva (a) before and (b) while it was exposed to a 5 s duration sound wave (200 Hz and 105 dB) in the pneumatic chip.

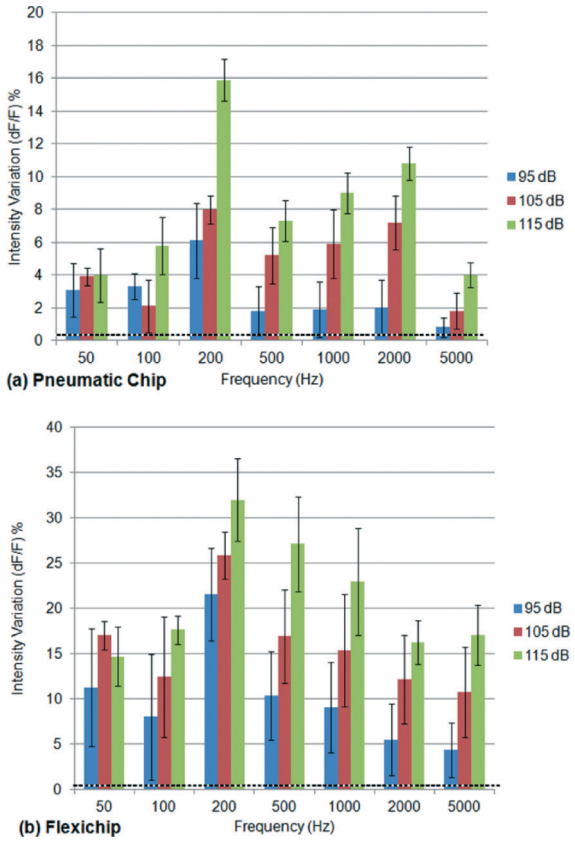

Fig. 8 CNS responses of fly larvae (n = 5) to various sound frequency and intensity levels tested inside (a) pneumatic chip and (b) FlexiChip. A peak in response at 200 Hz was observed in both chips with reduction in CNS activities when the frequency of the signal was decreased below or increased above 200 Hz. The increase in sound intensity resulted in the increase in CNS activities. The average response under no sound conditions was about 0.2% and 0.1% in the pneumatic chip and the FlexiChip, respectively. The error bars are one standard deviation from the mean.

between the peak frequency and the rest can be observed but is not statistically significant due to the lower signal to noise ratio (see the ESI† S3).

The level of mechanical vibrations induced by the sound waves at frequencies less than 50 Hz on the chip did not allow clear imaging of the CNS. The CNS response continued to decrease further beyond 5000 Hz (data not shown). The increase in sound intensity from 95 dB to 115 dB resulted in the corresponding increase in CNS activity. The increase in the sound level resulted in the reduction in the signal to noise ratio, indicating that the auditory response of the fly at a higher sound level was clearer.

In order to compare this method with other immobilization methods such as anesthetization, the response of 3rd instar larvae to pure tone sounds was measured before and after exposure to ether. The results indicate that the response to auditory stimulus was quite noticeably reduced in anesthetized larvae compared to the control sample, as shown in the ESI† (S1).

The peak observed in the CNS response at 200 Hz sound waves is in contrast to the recently reported observation that the optimal neuronal response to auditory stimulus in the larva occurs at 500 Hz. We noted two major differences between our experimental design and that used by Zhang *et al.*[23] First, in Zhang *et al.*,[23] the behavioral, calcium imaging and electrophysiological measurements involved the placement of the animals (or semi-intact preparations) directly on top of a speaker that delivered the auditory stimulus which may have coupled some of the vibrations to the larva as tactile stimulations. The use of whole body compression provides sufficient contact of the substrate to activate Cho sensory neurons that are spread throughout the body. Second, our devices exhibit physical separation of the speaker from the device, ensuring that it is the sound waves that cause the response while also providing a better simulation of sound cues that occur in nature. Since the larva is a burrowing animal, it is likely that the sensory neurons in the posterior abdominal segments are better tuned to a sound frequency that matches the wing beat frequency of the predatory wasp. We also test two different designs to separate any possible tactile stimulation effects.

4. Conclusions

With the availability of a new generation of reagents for monitoring neuronal activity through imaging and electrophysiological methods, it is necessary to develop custom engineered microdevices to facilitate experimental manipulations in intact-living specimens. We designed and evaluated two devices to anchor the *Drosophila* larval CNS so that stable optical recording of its neuronal activities could be conducted. The reduction in CNS movement was achieved through an on-chip mechanism that isolated the larval segments within which the CNS capsule is suspended. These microfluidic chips allowed us to stabilize the CNS specifically from ongoing motor movements and the resulting internal hemolymph displacements while the immobilization technique did not use any anaesthetic drugs which would affect animals' neurophysiological status. The pneumatic chip allowed automated animal loading, immobilization and unloading and it held the larva under positive fluid pressure to reduce the CNS movement entirely. However, since this is a closed-configuration chip, access of the larva to sound stimulation was indirect. The FlexiChip allowed for manual loading, unloading and immobilization. The posterior end of the larva inside the FlexiChip was open, thus allowing the larva to respire, and also for the acoustic vibrations to reach the larval body directly. The stability of the CNS inside both chips enabled the visualization of neuronal activities using a Genetically Encoded Calcium Indicator (GECI) probe, called GCaMP5, in response to auditory stimuli. Both chip designs allowed the stable recording of GCaMP5 fluorescence activity in the CNS. We report an optimal GCaMP5 response at 200 Hz. In conclusion, our customized larval lab-on-chip platforms allow the integration of functional imaging with a sensory-motor response. We anticipate that

our intact larva-on-a-chip will also be useful for other studies that involve calcium imaging as well as optogenetic and electrophysiological approaches.

Acknowledgements

The authors gratefully acknowledge financial support from the Natural Science and Engineering Research Council of Canada (NSERC) through their Discovery Program, The Canada Research Chairs Program and the Ontario Ministry of Research and Innovation through their Early Researchers Award.

Notes and references

1 S. Tickoo and S. Russell, *Curr. Opin. Pharmacol.*, 2002, **2**, 555–560.
2 S. Lenz, P. Karsten, J. B. Schulz and A. Voigt, *J. Neurochem.*, 2013, **127**, 453–460.
3 E. Bier, *Nat. Rev. Genet.*, 2005, **6**, 9–23.
4 J. B. Duffy, *Genesis*, 2002, **34**, 1–15.
5 H. Kohsaka, S. Okusawa, Y. Itakura, A. Fushiki and A. Nose, *Dev., Growth Differ.*, 2012, **54**, 408–419.
6 A. Schoofs, S. Niederegger, A. van Ooyen, H. Heinzel and R. Spiess, *J. Insect Physiol.*, 2010, **56**, 695–705.
7 S. Mondal, S. Ahlawat and S. P. Koushika, *J. Visualized Exp.*, 2012, **12**, 372–385.
8 P. Rezai, S. Salam, P. Selvaganapathy and B. P. Gupta, in *Integrated Microsystems*, ed. K. Iniewski, CRC Press, 2011, pp. 581–608.
9 S. E. Hulme and G. M. Whitesides, *Angew. Chem., Int. Ed.*, 2011, **50**, 4774–4807.
10 S. Mondal, S. Ahlawat, K. Rau, V. Venkataraman and S. P. Koushika, *Traffic*, 2011, **12**, 372–385.
11 M. Ghannad-Rezaie, X. Wang, B. Mishra, C. Collins and N. Chronis, *PLoS One*, 2012, **7**, e29869.
12 E. S. Heckscher, S. R. Lockery and C. Q. Doe, *J. Neurosci.*, 2012, **32**, 12460–12471.
13 T. V. Chokshi, A. Ben-Yakar and N. Chronis, *Lab Chip*, 2009, **9**, 151–157.
14 K. Chung, M. M. Crane and H. Lu, *Nat. Methods*, 2008, **5**, 637–643.
15 C. L. Gilleland, C. B. Rohde, F. Zeng and M. F. Yanik, *Nat. Protoc.*, 2010, **5**, 1888–1902.
16 F. Zeng, C. B. Rohde and M. F. Yanik, *Lab Chip*, 2008, **8**, 653–656.
17 J. R. Fakhoury, J. C. Sisson and X. J. Zhang, *Microfluid. Nanofluid.*, 2009, **6**, 299–313.
18 K. I. Wang, Z. Salcic, J. Yeh, J. Akagi, F. Zhu, C. J. Hall, K. E. Crosier, P. S. Crosier and D. Wlodkowic, *Biosens. Bioelectron.*, 2013, **48**, 188–196.
19 G. T. Dagani, K. Monzo, J. R. Fakhoury, C. C. Chen, J. C. Sisson and X. Zhang, *Biomed. Microdevices*, 2007, **9**, 681–694.
20 T. J. Levario, M. Zhan, B. Lim, S. Y. Shvartsman and H. Lu, *Nat. Protoc.*, 2013, **8**, 721–736.
21 E. M. Lucchetta, M. S. Munson and R. F. Ismagilov, *Lab Chip*, 2006, **6**, 185–190.
22 S. Zappe, M. Fish, M. P. Scott and O. Solgaard, *Lab Chip*, 2006, **6**, 1012–1019.
23 W. Zhang, Z. Yan, L. Y. Jan and Y. N. Jan, *Proc. Natl. Acad. Sci. U. S. A.*, 2013, **110**, 13612–13617.
24 T. Ohyama, T. Jovanic, G. Denisov, T. C. Dang, D. Hoffmann, R. A. Kerr and M. Zlatic, *PLoS One*, 2013, **8**, e71706.
25 J. Akerboom, T. W. Chen, T. J. Wardill, L. Tian, J. S. Marvin, S. Mutlu, N. C. Calderon, F. Esposti, B. G. Borghuis, X. R. Sun, A. Gordus, M. B. Orger, R. Portugues, F. Engert, J. J. Macklin, A. Filosa, A. Aggarwal, R. A. Kerr, R. Takagi, S. Kracun, E. Shigetomi, B. S. Khakh, H. Baier, L. Lagnado, S. S. Wang, C. I. Bargmann, B. E. Kimmel, V. Jayaraman, K. Svoboda, D. S. Kim, E. R. Schreiter and L. L. Looger, *J. Neurosci.*, 2012, **32**, 13819–13840.
26 Y. Xia and G. M. Whitesides, *Annu. Rev. Mater. Sci.*, 1998, **28**, 153–184.
27 A. H. Brand and N. Perrimon, *Development*, 1993, **118**(2), 401–415.
28 P. M. Salvaterra and T. Kitamoto, *Gene Expression Patterns*, 2001, **1**(1), 73–82.
29 J. Nakai, M. Ohkura and K. Imoto, *Nat. Biotechnol.*, 2001, **19**(2), 137–141.
30 J. Akerboom, J. D. Rivera, M. M. Guilbe, E. C. Malavé, H. H. Hernandez, L. Tian, S. Hires, J. S. Marvin, L. L. Looger and E. R. Schreite, *J. Biol. Chem.*, 2009, **284**(10), 6455–6464.
31 http://figshare.com/articles/FlexiChip1_0_A_simple_device_for_in_vivo_imaging_of_sensory_motor_activities_in_the_Drosophila_larval_CNS/644498.

